Current Biology 24, 29–39, January 6, 2014 ©2014 Elsevier Ltd All rights reserved http://dx.doi.org/10.1016/j.cub.2013.11.046

Article

KI Motifs of Human Knl1 Enhance Assembly of Comprehensive Spindle Checkpoint Complexes around MELT Repeats

Veronica Krenn,[1,2] Katharina Overlack,[1] Ivana Primorac,[1] Suzan van Gerwen,[1] and Andrea Musacchio[1,2,3,*]
[1]Department of Mechanistic Cell Biology, Max Planck Institute of Molecular Physiology, Otto-Hahn-Strasse 11, 44227 Dortmund, Germany
[2]Department of Experimental Oncology, European Institute of Oncology, Via Adamello 16, 20139 Milan, Italy
[3]Centre for Medical Biotechnology, Faculty of Biology, University of Duisburg-Essen, Universitätsstrasse, 45141 Essen, Germany

Summary

Background: The KMN network, a ten-subunit protein complex, mediates the interaction of kinetochores with spindle microtubules and recruits spindle assembly checkpoint (SAC) constituents to halt cells in mitosis until attainment of sister chromatid biorientation. Two types of motifs in the KMN subunit Knl1 interact with SAC proteins. Lys-Ile (KI) motifs, found in vertebrates, interact with the TPR motifs of Bub1 and BubR1. Met-Glu-Leu-Thr (MELT) repeats, ubiquitous in evolution, recruit the Bub3/Bub1 complex in a phosphorylation-dependent manner. The exact contributions of KI and MELT motifs to SAC signaling and chromosome alignment are unclear.

Results: We report here that KI motifs cooperate strongly with the neighboring single MELT motif in the N-terminal 250 residues ($Knl1^{1–250}$) of human Knl1 to seed a comprehensive assembly of SAC proteins. In cells depleted of endogenous Knl1, kinetochore-targeted $Knl1^{1–250}$ suffices to restore SAC and chromosome alignment. Individual MELT repeats outside of $Knl1^{1–250}$, which lack flanking KI motifs, establish qualitatively similar sets of interactions, but less efficiently.

Conclusions: MELT sequences on Knl1 emerge from our analysis as the platforms on which SAC complexes become assembled. Our results show that KI motifs are enhancers of MELT function in assembling SAC signaling complexes, and that they might have evolved to limit the expansion of MELT motifs by providing a more robust mechanism of SAC signaling around a single MELT. We shed light on the mechanism of Bub1 and BubR1 recruitment and identify crucial questions for future studies.

Introduction

Accurate chromosome segregation during mitosis and meiosis is accomplished by connecting chromosomes to the spindle, a microtubule-based structure [1]. The interactions of chromosomes with microtubules involve specialized protein assemblies named kinetochores [2, 3]. Kinetochores consist of at least 35 conserved protein core subunits and are organized as multilayered structures, with an inner kinetochore layer embedded in chromatin and an exposed outer kinetochore layer involved in microtubule binding.

*Correspondence: andrea.musacchio@mpi-dortmund.mpg.de

The Knl1 complex-Mis12 complex-Ndc80 complex (KMN) network, a ten-subunit protein assembly, is a crucial component of the outer kinetochore [4–13]. The "trunk" of the KMN network is the four-subunit Mis12 subcomplex (Mis12-C, also known as MIND or Mtw1 complex) [5–7, 9, 14, 15] (Figure 1A). By negative-stain electron microscopy (EM), the Mis12 complex appears as a cylinder with a long axis of ~22 nm [1, 17–19]. Its "roots" are embedded in the inner kinetochore through an interaction with CENP-C [2, 3, 20, 21], a conserved component of the constitutive centromere-associated network (CCAN) [4–13, 22]. From the Mis12 "trunk," two "branches" emerge, consisting of the four-subunit Ndc80 complex and the two-subunit Knl1 complex [5–7, 9, 14, 15, 17–19, 23]. The Ndc80 complex (Ndc80-C) takes the shape of a 55 nm dumbbell [24–26]. It harbors a microtubule-binding domain, located in the N-terminal region of the Ndc80 subunit, and is essential for the formation of load-bearing kinetochore-microtubule attachments [10, 24, 27, 28].

The Knl1 complex (Knl1-C, consisting of Knl1 and Zwint-1) has also been implicated in kinetochore-microtubule attachment [10, 29, 30] and plays a crucial regulatory function. Knl1 (also known as Spc105, Spc7, CASC5, AF15q14, and Blinkin), the largest subunit of the KMN network, contains an array of specialized sequence motifs (Figures 1B and 1C). A region of approximately 450 residues at the C terminus of Knl1 mediates the interaction with Zwint-1 and the Mis12 complex and is necessary and sufficient for kinetochore recruitment of Knl1 [17, 31–33]. At the other end of Knl1, the N-terminal 1,300 residues contain motifs that have been implicated in the regulation of the spindle assembly checkpoint (SAC), also known as mitotic checkpoint or metaphase checkpoint.

The SAC is a safety mechanism that coordinates the timing of mitotic exit with the completion of kinetochore-microtubule attachment [1, 34]. Its constituents become recruited to tensionless kinetochores, where they establish a network of protein-protein interactions that remain at least in part uncharacterized. This culminates in the formation of the mitotic checkpoint complex (MCC), the checkpoint effector, which targets the anaphase-promoting complex/cyclosome (APC/C) to prevent its ability to drive mitotic exit [1, 34].

With the possible exception of Aurora B, all SAC components, including Bub1, BubR1/Mad3, Bub3, Mad1, Mad2, Mps1, and the Rod-Zwilch-ZW10 complex, as well as the negative regulators of the SAC protein phosphatase 1 (PP1) and $p31^{comet}$, dock on the KMN network when recruited to kinetochores [31–33, 35–45]. Knl1 provides docking sites for several of these proteins. For instance, a PP1-binding domain in the N-terminal region of Knl1 (Figure 1A), which has also been implicated in microtubule binding, interacts with PP1 [29, 40, 46, 47]. Knl1 is also required for the recruitment of the Bub3/Bub1 complex (where Bub3 is a seven-WD40-repeat β-propeller and Bub1 is a kinase) and the Bub3/BubR1 complex (where BubR1 is a pseudokinase) [31, 32], which is in turn believed to support downstream SAC signaling events [1, 34].

Two short sequence motifs located near the N-terminal end of Knl1, known as KI1 and KI2 (Figures 1A and 1D), have been shown to interact with the TPR regions of Bub1 and BubR1, respectively [31, 33, 48, 49]. So far, KI1 and KI2 have been

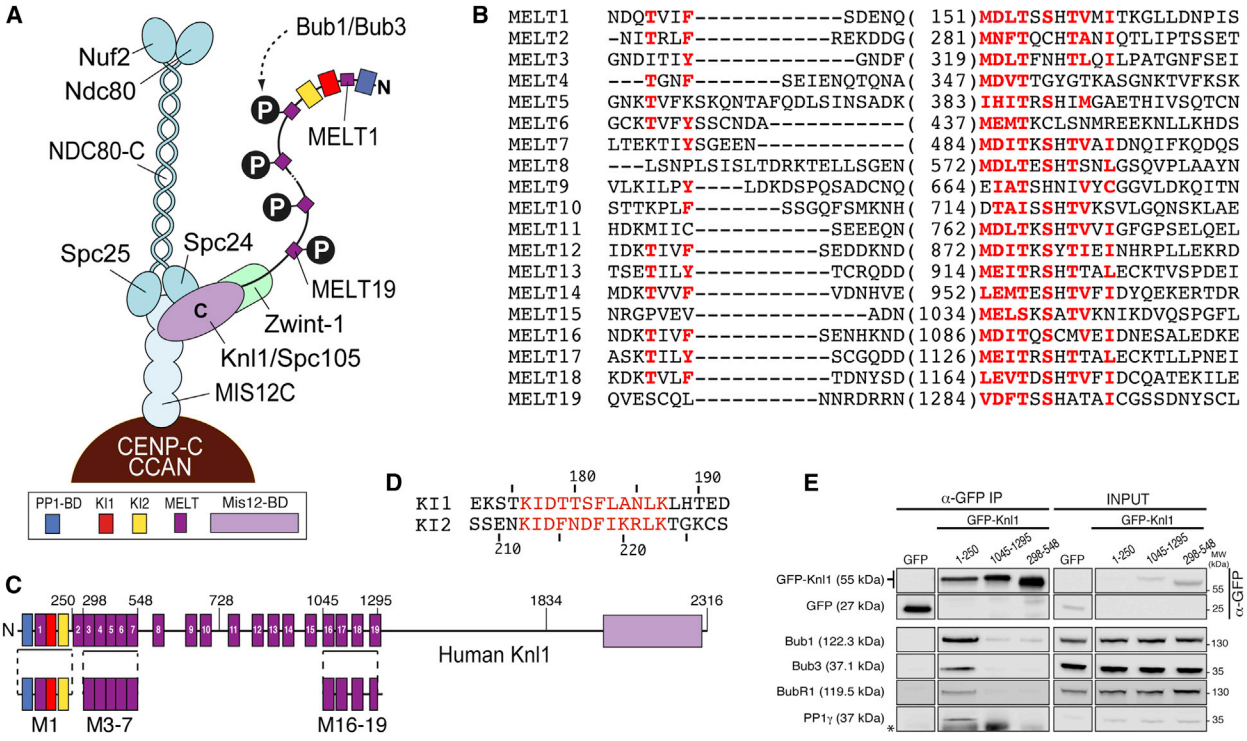

Figure 1. MELT and KI Motifs in Human Knl1

(A) Schematic depiction of the KMN network and of the recruitment of Bub1/Bub3 to the phosphorylated (P) MELT repeats of Knl1 at the kinetochore. Mps1 kinase (not shown) is responsible for MELT phosphorylation. N, N terminus; PP1-BD, protein phosphatase I binding domain; MIS12-BD, Mis12 binding domain.

(B) Alignment of 19 putative MELT repeats of human Knl1 showing conserved amino acids in bold red. Numbers refer to the position of the methionine (M) of each MELT sequence. An initial alignment generated with MEME [16] was complemented by manual scanning of the Knl1 sequence.

(C) Domain and motif organization of human Knl1. Relevant domain boundaries are indicated with residue numbers.

(D) Sequence of the KI1 and KI2 motifs of human Knl1 highlighted in red.

(E) Western blot showing immunoprecipitates (IPs) from ~6 mg mitotic lysates obtained from Flp-In T-REx HeLa stable cell lines expressing the indicated N-terminally tagged GFP-Knl1 constructs. The asterisk indicates a nonspecific signal. MW, molecular weight.

identified with confidence only in vertebrate Knl1 orthologs [33, 48]. KI1 and KI2 have been proposed to mediate the recruitment, respectively, of Bub3/Bub1 and of Bub3/BubR1 to Knl1 [31, 33]. However, mutations in the TPR domains of Bub1 and BubR1 that abolish their interaction with KI1 and KI2 do not overtly affect the localization of Bub1 and BubR1 [49]. Furthermore, KI1 and KI2 are not necessary for robust kinetochore recruitment of Bub1 and BubR1 [42], indicating that KI-TPR interactions are not crucial for Bub1 and BubR1 association with kinetochore-bound Knl1. The role of KI motifs in vertebrates has therefore remained unclear.

Other studies have identified the Bub3-binding domain of Bub1 (also named the GLEBS motif) as necessary and sufficient for robust kinetochore recruitment of Bub1 [49–51]. More recently, it was shown that crucial for kinetochore recruitment of Bub1 and Bub3 is their binding to the phosphorylated version of motifs that contain the consensus sequence [M/I/L/V]-[E/D]-[M/I/L/V]-T, where Thr in position 4 is the target of the SAC kinase Mps1 [42, 44, 45]. Such motifs, conserved in all organisms, are now generally referred to as MELT (the single-letter amino acid code for the sequence Met-Glu-Leu-Thr; we refer to the phosphorylated version of the motif as MELT^{P}), even if MELT is only a simplified consensus for a more complex sequence feature resulting from repeat expansions [12, 14, 43]. A plausible consensus for 19 identifiable MELTs in human Knl1 is shown in Figure 1B.

Preventing the phosphorylation of MELT motifs by mutating the crucial Thr at position 4 in most or all MELT repeats results in a checkpoint defect both in *S. cerevisiae* and in *S. pombe* [42, 44, 45]. The recent crystal structure of a synthetic MELT^{P} peptide in complex with Bub3 and with the Bub3-binding domain of Bub1 identified an extraordinarily well-conserved region on the side of the seven-WD40 β-propeller of Bub3 as the MELT^{P} receptor [52]. The ability of Bub3 to recognize MELT^{P} is required for kinetochore recruitment of Bub1 and for the checkpoint response in *Saccharomyces cerevisiae* [52].

Collectively, these very recent findings provide a rather detailed description of the mechanism through which phosphorylated MELT motifs promote the recruitment of the Bub1/Bub3 complex. However, how recruitment of Bub3/Bub1 to MELT motifs can promote downstream events of checkpoint signaling, such as Bub3/BubR1 recruitment, is not known. Additionally, whether multiple MELT repeats are redundant or act additively is unclear. Furthermore, the role of the KI1 and KI2 motifs of Knl1 in vertebrates has not been clarified. To answer some of these questions, we carried out a detailed analysis on the first 250 residues of human Knl1, a region that is especially dense in functional sequence motifs, including a PP1-binding site, a MELT motif, and the consecutive KI1 and KI2 motifs. Our data indicate that MELT motifs are platforms for the assembly of comprehensive SAC complexes, and that the KI1 and KI2 motifs are MELT enhancers.

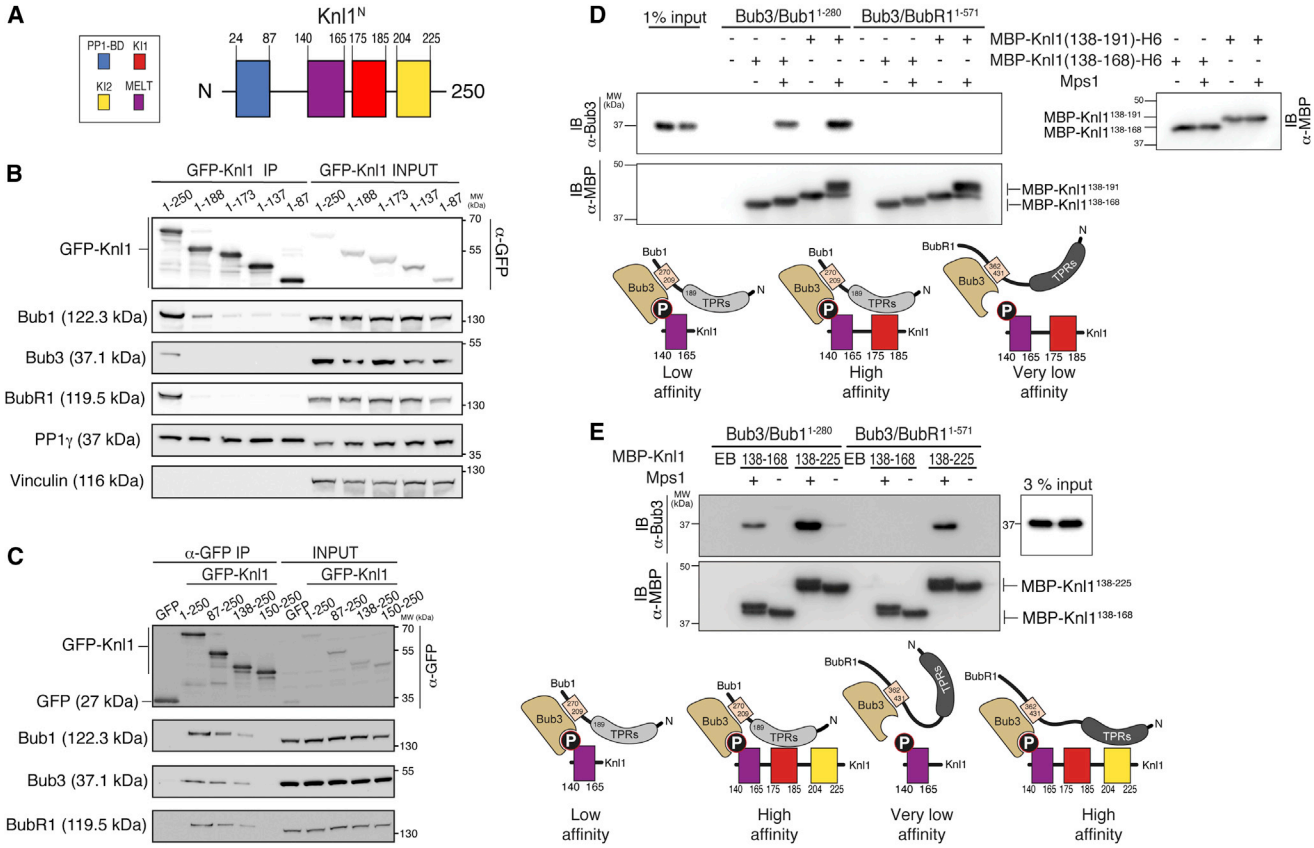

Figure 2. Molecular Determinants of Tight Binding of Bub1 and BubR1 to Knl1$^{1–250}$

(A) Schematic description of the motif organization of the first 250 residues of human Knl1 (Knl1^{N}).

(B and C) Western blotting of immunoprecipitates from ~3.3 mg (A) or ~3.0 mg (B) mitotic lysates from Flp-In T-REx stable cells expressing the indicated N-terminally tagged GFP-Knl1 constructs carrying C-terminal (B) or N-terminal (C) deletions. Vinculin was used as loading control.

(D) Recombinant Bub3/Bub1$^{1–280}$ complexes or Bub3/BubR1$^{1–571}$ complexes (at 400 nM concentration) were incubated with immobilized MBP fusions of the indicated Knl1 fragments prephosphorylated with Mps1 (+) or unphosphorylated (−). The blot is representative of five independent experiments. The western blot on the right shows the amounts of MBP fusion proteins in each reaction before addition of ATP. The schemes under the gels summarize the binding mechanism. The Bub3-binding domain (also known as GLEBS) of Bub1 or BubR1 is represented as a pink rectangle associated with the Bub3 β-propeller. N, N terminus; BD, binding domain; MW, molecular weight; KD, kinase domain; IB, immunoblot. The two lanes marked as "input" were loaded with Bub3/Bub1$^{1–280}$ (left) or Bub3/BubR1$^{1–571}$ (right).

(E) Recombinant Bub3/Bub1$^{1–280}$ or Bub3/BubR1$^{1–571}$ complexes (at 400 nM concentration) were incubated with immobilized MBP fusions of the indicated Knl1 fragments prephosphorylated with Mps1 (+) or unphosphorylated (−). Lanes indicated as EB show lack of background binding to empty beads. N, N terminus; BD, binding domain; MW, molecular weight; IB, immunoblot, MBP, maltose-binding protein.

Results

We have previously shown that the interaction of the KI1 and KI2 motifs of Knl1 with Bub1 and BubR1 is dispensable for robust kinetochore recruitment of these SAC proteins [49]. However, as KI motifs are located close to MELT repeats, we hypothesized that KI1 and KI2 motifs, by binding to the TPR domains of Bub1 and BubR1, might enhance the affinity of the Bub3/Bub1 and Bub3/BubR1 complexes for Knl1. To test this idea, we resorted to immunoprecipitation (IP), a typical nonequilibrium assay, and used it to address the persistence of bound complexes. We created expression constructs in which Knl1$^{1–250}$, Knl1$^{298–548}$, and Knl1$^{1045–1295}$, containing respectively MELT1 only and the KI motifs, MELT3 to MELT7, and MELT16 to MELT19 (Figure 1C), were fused to GFP. We then expressed these proteins in HeLa cells and pulled them down from lysates of mitotic cells with an anti-GFP antibody. After extensive washing, we probed the precipitates with antibodies against Bub1, Bub3, BubR1, and PP1γ (Figure 1E). In agreement with the hypothesis that the KI motifs contribute to the robustness of the interaction of Bub1, Bub3, and BubR1 with MELT1^{P}, GFP-Knl1$^{1–250}$ pulled down considerably larger amounts of Bub1, Bub3, and BubR1 compared to GFP-Knl1$^{298–548}$ and GFP-Knl1$^{1045–1295}$ (note that PP1γ, which was also pulled down by GFP-Knl1$^{1–250}$, was expected to interact exclusively with GFP-Knl1$^{1–250}$, the segment of Knl1 that contains the phosphatase binding site). Thus, the interaction of Bub1, BubR1, and Bub3 with a single MELT repeat flanked by the KI1 and KI2 motifs is significantly more persistent than with other Knl1 segments containing multiple MELT motifs.

Molecular Determinants of Tight Binding of Bub1 and BubR1 to Knl1$^{1–250}$

To probe the contribution of the KI motifs to the interactions mediated by the Knl1$^{1–250}$ construct, we created two series of deletion mutants of Knl1$^{1–250}$ (the organization of motifs in this region is summarized in Figure 2A) as N-terminally GFP-tagged proteins in which progressively larger segments of

Knl1 were removed from the N or the C terminus. After precipitation from lysates of mitotic HeLa cells with an anti-GFP antibody, western blotting was used to assess the abundance of Bub1, Bub3, and BubR1 associated with each construct. As shown above in Figure 1E, GFP-Knl1$^{1–250}$ efficiently pulled down Bub1, Bub3, and BubR1. Deletions from the C terminus removing KI2 but leaving an intact MELT and KI1 (GFP-Knl1$^{1–188}$) prevented BubR1 binding but also caused a strong reduction in the amounts of bound Bub1 (Figure 2B). Because KI2 has been shown to bind BubR1 but not Bub1 in reconstitution experiments in vitro [33, 48, 49], this experiment suggests that binding of BubR1 through the KI2 motif stabilizes the interaction of Bub1 with the neighboring MELT1-KI1 motifs. Upon additional removal of the KI1 motif (GFP-Knl1$^{1–173}$), the amounts of bound Bub1 were further reduced (Figure 2B). All constructs contained an intact N-terminal PP1 binding site and consistently bound PP1 to similar levels.

Next, we tested the effects of N-terminal deletions. Removal of 86 or 137 residues (GFP-Knl1$^{87–250}$ and GFP-Knl1$^{138–250}$), both of which preserve the combination of MELT1, KI1, and KI2, resulted in a significant but relatively modest decrease in the amounts of Bub1, Bub3, and BubR1 bound to the GFP-Knl1 baits. Further deletion of 12 residues (GFP-Knl1$^{150–250}$), which affected the integrity of MELT1 but not of KI1 and KI2, resulted in the reduction of Bub1, Bub3, and BubR1 to background levels (Figure 2C).

Collectively, these results demonstrate that both the MELT1 and the KI1 and KI2 motifs of Knl1$^{1–250}$ are instrumental for tight binding of Bub1, Bub3, and BubR1. The exact catalog of interactions between these proteins is likely complex and currently unclear. We imagined that cooperative interactions might arise if the Bub3/Bub1 or Bub3/BubR1 complexes interacted simultaneously with the MELT1^{P}-KI1 or MELT1^{P}-KI2 constellation of Knl1, respectively. We started testing this by comparing the ability of recombinant Bub3/Bub1$^{1–280}$ or Bub3/BubR1$^{1–571}$ (containing both the TPR and the Bub3-binding domain of Bub1 and BubR1, respectively), previously purified to homogeneity, to interact with MBP-Knl1$^{138–168}$ (MELT1 only) or MBP-Knl1$^{138–191}$ (MELT1 + KI1) immobilized in solid phase. To test the dependence of the interactions on Mps1 phosphorylation, we treated half of the immobilized MBP-Knl1 fusion proteins with Mps1 kinase (Figure 2D). At a concentration of 400 nM, Bub3/Bub1$^{1–280}$ bound Knl1$^{138–168}$ or Knl1$^{138–191}$ in a phosphorylation-dependent manner, suggesting that the interaction is at least in part mediated by the binding of the Bub3 β-propeller of Bub3 to the phosphorylated MELT1 [42, 44, 45, 52]. However, Bub3/Bub1$^{1–280}$ bound to MBP-Knl1$^{138–191}$ with significantly higher affinity in comparison to MBP-Knl1$^{138–168}$ (Figure 2D), strongly suggesting the existence of a concomitant interaction of the TPR domain of Bub1 with KI1. Similar results were obtained when Bub3/Bub1$^{1–280}$ was incubated with MBP-Knl1$^{138–225}$, a segment that contains both KI1 and KI2 (Figure 2E). In all cases, Mps1 activity was required for the interactions.

These observations suggest that binding of the TPR of Bub1 to KI1, concomitantly with the binding of the β-propeller of Bub3 to MELT1^{P} [52], enhances the affinity of Bub3/Bub1$^{1–280}$ for Knl1 cooperatively. Conceptually similar results were observed when we incubated Bub3/BubR1$^{1–571}$ with the MBP-Knl1 constructs (Figures 2D and 2E), but one important difference emerged: Bub3/BubR1$^{1–571}$ (at 400 nM) was not able to interact with MBP-Knl1$^{138–168}$ or MBP-Knl1$^{138–191}$, the two constructs lacking KI2, regardless of the presence of phosphorylation. This was specific to the Bub3/BubR1$^{1–571}$ construct because, as shown above, Bub3/Bub1$^{1–280}$ (at the same concentration) bound MBP-Knl1$^{138–168}$ in a phosphorylation-dependent manner (Figures 2D and 2E). This observation suggests that unlike Bub1, BubR1 suppresses the ability of Bub3 to interact with phosphorylated MELT repeats, as postulated recently [52]. It also agrees with the previous observation that the BubR1 TPR domain does not bind KI1 [49].

Bub3/BubR1$^{1–571}$, however, interacted with MBP-Knl1$^{138–225}$ in a phosphorylation-dependent manner (Figure 2E). This result shows that the interaction of the BubR1 TPR with KI2 enhances the binding affinity of Bub3/BubR1$^{1–571}$ for MBP-Knl1$^{138–225}$. Moreover, the phosphorylation dependence of the interaction indicates that the ability of the Bub3 propeller to interact with phosphorylated motifs is not completely abolished in the Bub3/BubR1 complex but only partly suppressed. Our binding models in Figures 2D and 2E incorporate the previous finding that Bub1 and BubR1 TPRs bind selectively to their cognate KI1 and KI2 motifs, respectively [49]. Collectively, these results indicate that the presence of MELT1 is necessary but not sufficient for a tight interaction of Bub1, Bub3, and BubR1 with the Knl1$^{1–250}$ construct, and that KI1 and KI2 strongly enhance the potency of the interaction with Bub3/Bub1 and Bub3/BubR1.

MELT Motifs Assemble SAC Complexes

To shed light on the consequences of the recruitment of Bub1, BubR1, and Bub3 to Knl1, we precipitated GFP-Knl1$^{1–250}$ and analyzed the resulting precipitates by western blotting to assess whether other SAC components were present. Remarkably, besides Bub1 and BubR1, we identified in Knl1$^{1–250}$ precipitates all SAC proteins, including Mps1, Mad1, Mad2, and Cdc20. Additionally, we detected the APC/C subunit APC7 (Figures 3A and 3B).

To assess whether Bub1 was required for these interactions, we repeated the precipitation experiments from lysates of cells in which Bub1 had been depleted by RNA interference (Figure 3C). In agreement with the prediction that Bub1 is necessary for the assembly of SAC complexes on Knl1$^{1–250}$, the levels of Bub3, BubR1, Cdc20, and to a lesser extent Mps1 were severely affected by Bub1 depletion (Figure 3C). When considered together with the results in Figure 2, these results indicate that Knl1$^{1–250}$ acts as a platform for the assembly of checkpoint complexes by initiating the recruitment of Bub3/Bub1 complexes, which further recruits Bub3/BubR1 and additional downstream components. The results also strongly suggest that Bub1 and BubR1 bind concomitantly and noncompetitively to Knl1$^{1–250}$ and that BubR1 stabilizes the binding of Bub1, possibly through cooperative interactions, as discussed more thoroughly in the next section.

Kinetochore Targeting Enhances Interactions of Knl1$^{1–250}$

Next, we tested whether Knl1$^{1–250}$ was able to interact with Bub1, Bub3, and BubR1 also when targeted to kinetochores. For this, we fused its coding sequence to that of the C-terminal kinetochore-targeting domain of Knl1 (residues 1834–2316) and a C-terminal GFP (Knl1$^{1–250+C}$-GFP). The isolated C-terminal domain of Knl1 (Knl1^{C}-GFP) was used as a positive control for kinetochore localization (Figure 4A). The resulting constructs were integrated at a single genomic locus in HeLa cells, from which their expression was induced by addition of doxycycline [53] (see Figure S1 available online).

In IP experiments, we found that the targeting of Knl1$^{1–250}$ to kinetochores by fusion to the Knl1 C-terminal domain (Knl1$^{1–250+C}$) strongly enhanced its interactions with Bub1, Bub3, and BubR1 (Figure 4B) compared to the soluble

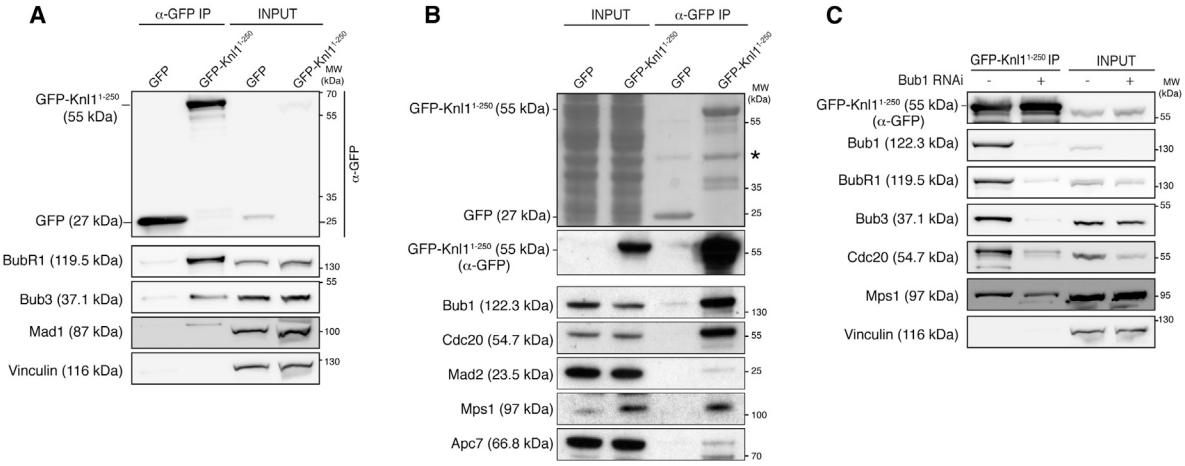

Figure 3. MELT Motifs Assemble Spindle Assembly Checkpoint Complexes

(A and B) Western blot showing immunoprecipitates from ~10 mg (A) or ~4 mg (B) mitotic lysates obtained from Flp-In T-REx stable cells expressing GFP or GFP-Knl1$^{1–250}$. The top panel in (B) shows the membrane stained with Ponceau. The asterisk indicates a protein that binds nonspecifically to GFP-Trap beads during the immunoprecipitation. Vinculin was used as loading control.

(C) Western blot showing immunoprecipitates from ~10 mg mitotic lysates obtained from Flp-In T-REx stable cells expressing GFP-Knl1$^{1–250}$ after depletion of Bub1 by RNAi and treatment with 330 nM nocodazole for 5 hr. Vinculin was used as loading control. MW, molecular weight.

Knl1$^{1–250}$ construct, possibly a consequence of more efficient Mps1 phosphorylation at the kinetochore. No binding of Bub1, Bub3, and BubR1 could be detected in the IP of Knl1^{C}-GFP. Kinetochore targeting was confirmed by concomitant IP of other KMN subunits, including Mis12, Hec1, and Zwint-1 (Figure 4B). In agreement with our prediction in the previous paragraph, Bub1 and BubR1 were mutually supporting their interaction with the Knl1 N-terminal region at kinetochores (Figure S2A).

Next, we compared the ability of Knl1$^{1–250+C}$ to pull down Bub1, Bub3, and BubR1 to that of a larger Knl1 fragment containing multiple MELT repeats in addition to the KI motifs. We therefore used a fragment corresponding to residues 1–728 of Knl1, which has been previously shown to be sufficient for a robust checkpoint response in the absence of endogenous Knl1 [33]. With its ten MELT motifs, Knl1$^{1–728+C}$ was able to pull down significantly larger amounts of Bub1, Bub3, and BubR1 compared to Knl1$^{1–250+C}$ (Figure 4C; note that the apparent lack of Bub3 in the IPs with Knl1$^{1–250+C}$ in this figure is due to the apparently nonlinear response of the Bub3 antibody in western blots, as illustrated in Figure S2B). Similar levels of Mis12 were present in the precipitates, indicating that all proteins had reached kinetochores effectively.

By removing the MELT1-KI1-KI2 region (Δ138–250) (Figure S2C), we determined that Knl1$^{1–728(Δ138–250)+C}$-GFP was approximately as efficient as Knl1$^{1–250+C}$ in pulling down Bub1, BubR1, and Bub3 in IP assays (Figures S2D and S2E). These differences were unlikely to be caused by a differential interaction of the deletion constructs with PP1 phosphatase, as we have shown that the latter was present at similar levels in precipitates of different Knl1 N-terminal segments (Figure 2A). Thus, the constellation of MELT1-KI1-KI2 is approximately as efficient as an array containing MELT2 to MELT10 in pulling down Bub3/Bub1 and Bub3/BubR1.

Knl1$^{1–250}$ at the Kinetochore Is Sufficient for a Robust Checkpoint Response

We next asked whether Knl1$^{1–250+C}$ was sufficient for a checkpoint response in cells depleted of endogenous Knl1. The Knl1$^{1–250+C}$ construct, as well as Knl1^{C} and Knl1$^{1–728+C}$ described in the previous paragraph (and derivatives described later), was siRNA resistant and was expressed in cells depleted of endogenous Knl1 at the levels shown in Figure S1A. The constructs localized robustly to kinetochores in the absence of endogenous Knl1 (Figure S1B). Elimination of endogenous Knl1 by RNA interference was quite efficient, as judged by western blotting and fluorescence microscopy (Figures S1A and S1B).

In cells depleted of Knl1, Knl1$^{1–728+C}$ was able to restore significant kinetochore levels of Bub1 and BubR1. Further deletion of residues 138–250 from Knl1$^{1–728+C}$ (Knl1$^{1–728(Δ138–250)+C}$-GFP) did not affect the levels of Bub1 in comparison to those observed in Knl1$^{1–728+C}$-expressing cells but led to a significant reduction of the levels of BubR1 (Figures S3B and S3C). Conversely, little Bub1 and BubR1 were visible on kinetochores of cells expressing the Knl1$^{1–250+C}$ or Knl1^{C} constructs (Figure 5A; Figure S3A). With a single MELT repeat, Knl1$^{1–250+C}$ is likely to bind to single Bub1 and BubR1 molecules, possibly explaining why their levels do not exceed the detection threshold (for Bub1) or do so only moderately (for BubR1). In agreement with this hypothesis, we show that Knl1$^{1–250}$ was able to recruit detectable levels of Bub1 and BubR1 when targeted to centrosomes as a fusion to the Plk4-centrosome-targeting domain, which provides abundant docking sites at centrosomes (Figure S4). Alternatively, the Bub1 and BubR1 epitopes recognized by the antibodies used in this study might be masked when Bub1 and BubR1 are bound to Knl1$^{1–250}$ in a complex with the other SAC proteins.

We next asked whether Knl1$^{1–250}$ was able to sustain the SAC when targeted to kinetochores in cells depleted of endogenous Knl1. HeLa cells depleted of endogenous Knl1 were still able to mount a relatively robust checkpoint response in the presence of spindle poisons (330 nM nocodazole). This phenotype is likely to reflect incomplete Knl1 depletion, as suggested previously [31, 33]. Because the combination of RNAi-based depletion of kinetochore subunits with the addition of SAC inhibitors has been shown to have strong synergistic negative effects on SAC function [54, 55], we added a

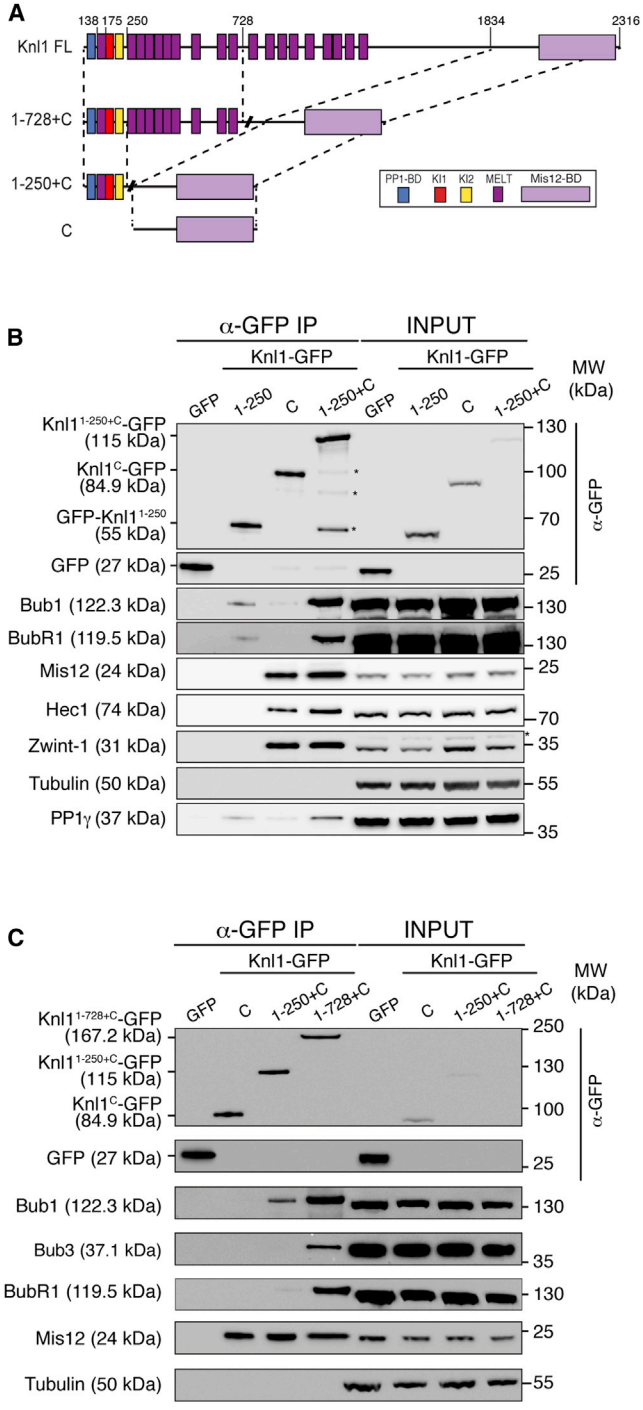

Figure 4. Kinetochore Targeting Enhances Interactions of Knl1$^{1–250}$

(A) Schematic representation of Knl1 chimeras used in this figure. FL, full length. C, C-terminal domain (residues 1834–2316).

(B) Western blot of immunoprecipitates from ~5 mg mitotic lysates obtained from Flp-In T-REx stable cells expressing the indicated Knl1-GFP constructs. Note that the Knl1$^{1–250}$ construct is N-terminally GFP-tagged, whereas the others carry the tag at their C terminus. Tubulin was used as loading control. Asterisks indicate degradation products.

(C) Western blot of immunoprecipitates from ~4.2 mg mitotic lysates obtained from Flp-In T-REx stable cells expressing the indicated Knl1-GFP constructs. Tubulin was used as loading control. MW, molecular weight; BD, binding domain.

suboptimal concentration of the SAC inhibitor reversine [56] to exacerbate the expected checkpoint defect of Knl1-depleted cells in the presence of nocodazole (Figure 5B; Figure S5A).

In the presence of 330 nM nocodazole and 250 nM reversine, cells expressing the C-terminal domain of Knl1 (Knl1^{C}) were not able to mount a checkpoint response, as shown previously [33] (Figure 5B). Interestingly, expression of Knl1$^{1–250+C}$-GFP was sufficient to rescue the checkpoint response in Knl1-depleted cells to levels similar to those of control depletion and the Knl1$^{1–728+C}$-GFP construct (Figure 5B). Thus, the first 250 residues of Knl1 contain sufficient sequence information to mount a strong checkpoint response in cells treated with spindle poisons and suboptimal concentrations of a checkpoint inhibitor. Very similar results were obtained when combining paclitaxel and reversine (data not shown).

We also monitored the ability of different Knl1 constructs to complement the alignment defect caused by depletion of Knl1 (Figure 5C). In this assay, the Knl1^{C}-GFP construct, expressing only the C-terminal kinetochore-targeting region of Knl1, dramatically exacerbated the negative effects of partial Knl1 depletion on chromosome alignment, as observed previously [33]. Cells expressing Knl1$^{1–250+C}$-GFP or Knl1$^{1–728+C}$-GFP displayed a marked improvement in chromosome alignment in comparison to cells expressing only the C-terminal domain, with Knl1$^{1–728+C}$-GFP being more effective than Knl1$^{1–250+C}$-GFP (Figure 5C). Altogether, these results demonstrate that kinetochore localization of the first 250 residues of Knl1, which contain a single MELT repeat and KI motifs, can sustain the checkpoint response effectively. Knl1$^{1–250+C}$-GFP also supports chromosome alignment, albeit less efficiently than Knl1$^{1–728\ +C}$. Depletion of residues 138–250 only mildly decreased the checkpoint and alignment response of Knl1$^{1–728+C}$-GFP (Figures S5B and S5C), as expected from the biochemical analysis.

Robust SAC and Alignment Functions of Knl1$^{1–250}$ Require KI1 and KI2

Finally, we asked whether the ability of Knl1$^{1–250+C}$-GFP to support SAC and chromosome alignment required the presence of KI motifs. We therefore introduced point mutations at residues previously implicated in the interaction with Bub1 and BubR1 [48, 49], in the context of Knl1$^{1–250+C}$+C (Figure 6A). We refer to the resulting mutant as Knl1$^{1–250\text{-}KI1+2/AAA+C}$. In IP experiments, Knl1$^{1–250\text{-}KI1+2/AAA+C}$ displayed strongly reduced binding to Bub proteins (Figures 6B and 6C; note that the quantification of Bub3 in Figure 6C might suffer from the relatively low signals of Bub3). We obtained only a partial checkpoint response in cells expressing Knl1$^{1–250\text{-}KI1+2/AAA+C}$ compared to wild-type Knl1$^{1–250+C}$ (Figure 6D), indicating that the presence of intact KI1 and KI2 motifs affects the functional integrity of Knl1$^{1–250}$, albeit not completely. A similarly reduced checkpoint response was observed in cells expressing Knl1$^{1–250\text{-}\Delta175\text{-}225+C}$, which lacks KI1 and KI2 (Figure S5D). Further deletion of the MELT1 sequence (Knl1$^{1–250\text{-}\Delta138–225+C}$) essentially abrogated the checkpoint response observed with Knl1$^{1–250+C}$ (Figure S5D). The KI1 and KI2 motifs were also important for chromosome alignment, as Knl1$^{1–250\text{-}KI1+2/AAA+C}$ was unable to overcome the negative effects on alignment deriving from the expression of the Knl1 C-terminal region (Figure 6E). Collectively, these observations point to an important role of the KI1 and KI2 motifs in determining the remarkable robustness of Knl1$^{1–250+C}$ in the checkpoint and alignment response.

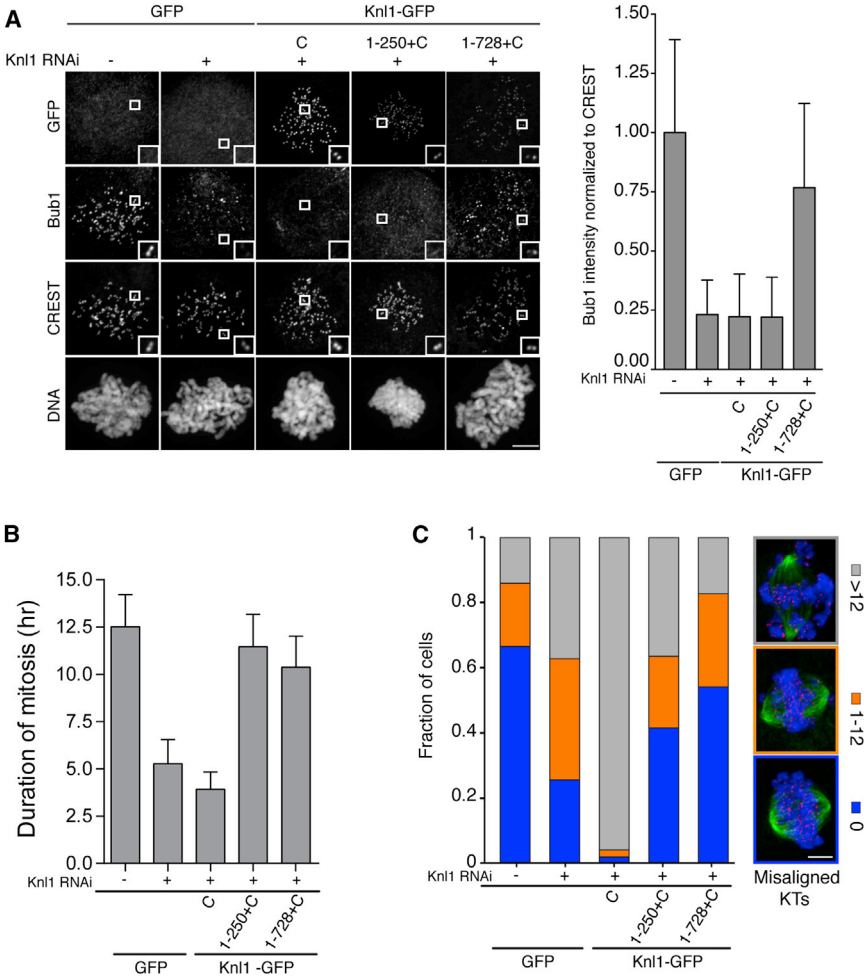

Figure 5. Knl1$^{1–250}$ at the Kinetochore Is Sufficient for a Robust Checkpoint Response

(A) Left: representative images of Flp-In T-REx HeLa stable cells expressing the indicated Knl1-GFP proteins after treatment with nocodazole for 4 hr. CREST was used to visualize centromeres. Insets show a higher magnification of kinetochore regions (indicated by boxes). Right: quantification of Bub1 kinetochore levels normalized to the CREST kinetochore. The graph shows mean intensities from one representative experiment out of two. The mean value for nondepleted cells is set to 1. Error bars indicate SD. Scale bar represents 5 μm.

(B) Mean duration of mitosis of Flp-In T-REx stable cells expressing various Knl1-GFP constructs in the presence of 330 nM nocodazole and 250 nM reversine. Cell morphology was used to measure entry into and exit from mitosis by time-lapse microscopy (n > 175 from three independent experiments). Error bars represent SEM.

(C) Quantification of chromosome alignment in Flp-In T-REx stable cells expressing the indicated Knl1-GFP constructs after treatment with 5 μM MG132 for 4 hr. Immunostaining shows tubulin in green, centromeres (CREST) in red, and DNA in blue. The graph shows the fraction of cells (n > 155 from two independent experiments). KTs, kinetochores. Scale bar represents 5 μm.

Discussion

Knl1 has emerged in recent years as a crucial platform for checkpoint signaling at the kinetochore [1, 34]. Especially important was the identification of the nearly ubiquitous MELT repeats of Knl1 as crucial sites for kinetochore binding of the Bub3/Bub1 complex [42, 44, 45]. In a recent study, we showed that synthetic peptides encompassing a single MELT repeat from *Saccharomyces cerevisiae* engage in interactions with recombinant Bub3/Bub1 with dissociation constants in the submicromolar range [52]. The data presented here, although unsystematic, are consistent with the view that MELT repeats in human Knl1 act as single and independent recruitment models to recruit Bub3/Bub1 complexes in an additive fashion. Sequence variation around the conserved consensus of the numerous MELT repeats present in human Knl1 may influence their binding affinity for Bub3/Bub1. Understanding whether individual MELTs have different affinities for Bub3/Bub1 and the identification of determinants for such differences will require a more systematic analysis of MELT-Bub3/Bub1 interactions.

Here, we have shown that a single MELT motif and its neighboring KI motifs act as a platform for the assembly of comprehensive SAC complexes. This region of Knl1 was sufficient for robust SAC signaling and chromosome alignment when recruited to the kinetochore through a fusion to the C-terminal kinetochore-targeting domain. Although we have tested only the combination of KI1 and KI2 with MELT1 in our studies, it is possible that other MELT sequences can also cooperate with KI1 and KI2 motifs. Previously, a construct fusing the N-terminal 588 residues to a C-terminal domain of the *Drosophila melanogaster* Knl1 ortholog DmSpc105 was also shown to rescue the deficiency of a null allele of Spc105 [43]. The central domain of *Drosophila* Spc105 contains several copies of a repeat whose consensus does not conform to the MELT sequence, but at least two MELT-like motifs are present in the N-terminal region (at residues 210–213 and 312–315). Furthermore, KI1 and KI2 motifs have not been identified with certainty in this organism. In light of these important sequence differences, it is difficult to relate these previous observations to the ones presented here.

We have demonstrated that the KI1 and KI2 motifs act as MELT enhancers by stabilizing Bub3/Bub1 binding to MELT1. The unique combination of sequence motifs allows the N-terminal region of Knl1 to establish robust interactions with Bub1, Bub3, and BubR1. Our studies with recombinant proteins suggest strongly that the special behavior of the N-terminal region of human Knl1 stems from cooperative interactions of different domains and motifs in Knl1, Bub3/Bub1, Bub3/BubR1, and possibly other checkpoint components. These concepts are summarized in Figure 7.

Collectively, our results provide a molecular explanation for our previous observation that mutations in the KI1-binding region of the Bub1 TPR domain weaken the interaction of the mutated Bub1 with kinetochore subunits in IP assays [49]. It might seem puzzling that the same Bub1 mutants decorated kinetochores to levels that were indistinguishable from those of wild-type Bub1 [49]. We suspect that at its steady-state

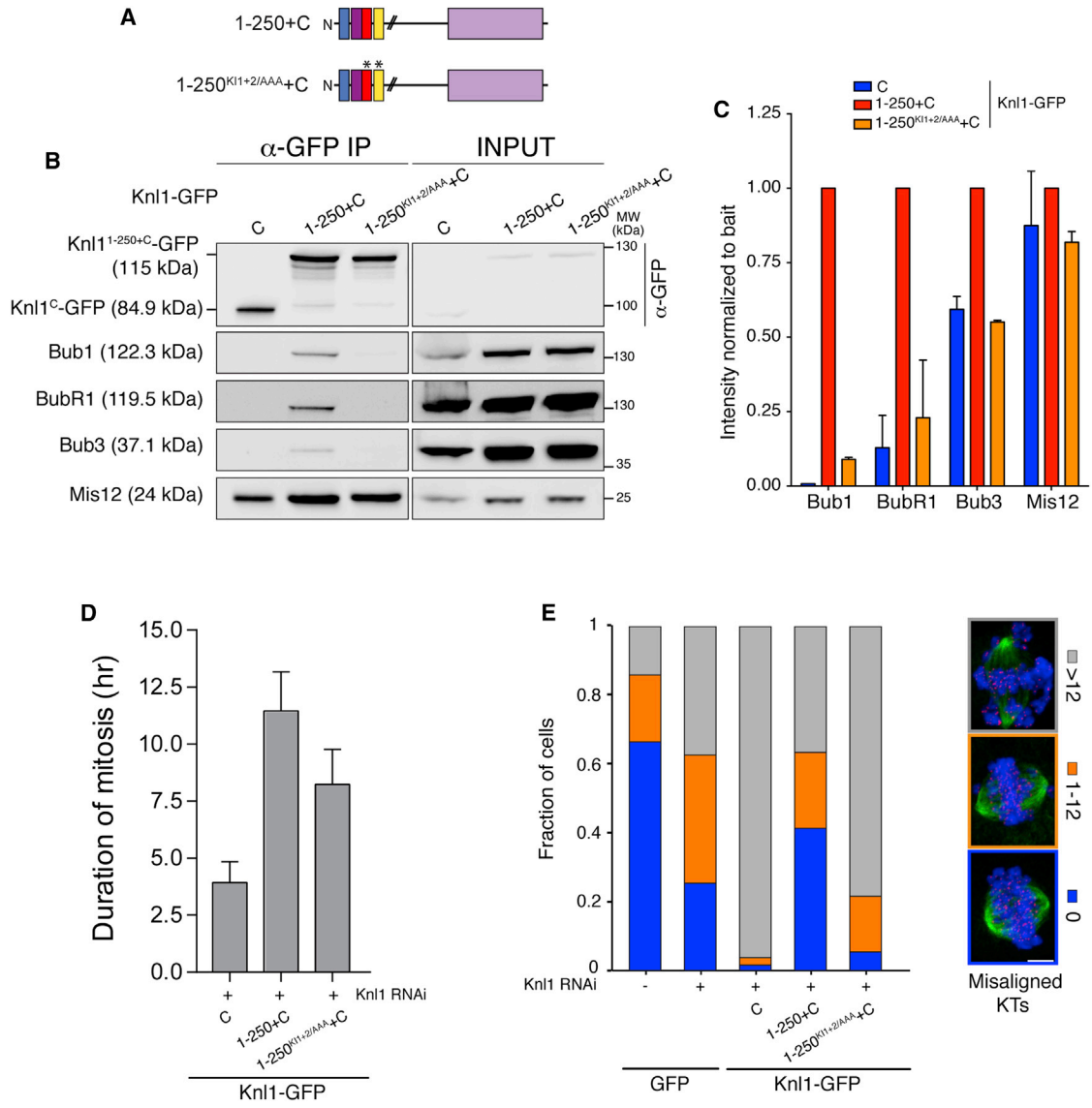

Figure 6. Robust Spindle Assembly Checkpoint and Alignment Mediated by Knl1$^{1–250}$ Require KI1 and KI2

(A) Schematic representation of Knl1-GFP chimeras. Asterisks indicate alanine mutations introduced in the KI motifs. Specifically, each residue in the K-I-D motif of KI1 and KI2 was mutated into alanine (indicated as KI1+2/AAA).

(B) Western blot showing immunoprecipitates from ~4.2 mg mitotic lysates obtained from Flp-In T-REx stable cells expressing the indicated Knl1-GFP constructs.

(C) Quantification of the western blot in (B). The amounts of coimmunoprecipitating Bub1, BubR1, Bub3, and Mis12 proteins were normalized for the amount of Knl1-GFP proteins present in the IP. Values for the control Knl1$^{1–250+C}$-GFP construct are set to 1. The graph shows the mean intensity of two independent experiments. Error bars represent SEM.

(D) Graph representing the mean duration of mitosis in Flp-In T-REx HeLa stable cell lines expressing the indicated Knl1-GFP constructs in the absence of endogenous Knl1 and in the presence of 330 nM nocodazole and 250 nM reversine. Cell morphology was used to measure entry into and exit from mitosis by time-lapse microscopy (n > 175 from three independent experiments). Error bars represent SEM. Note that the values of the control constructs are the same as shown in Figure 5B.

(E) Chromosome alignment of Flp-In T-REx stable cells expressing the indicated Knl1-GFP constructs after treatment with 5 μM MG132 for 4 hr. Immunostaining shows tubulin in green, centromeres (CREST) in red, and DNA in blue. The graph shows the fraction of cells (n > 155 from two independent experiments). The values of control constructs and representative images are the same as shown in Figure 5C. MW, molecular weight. Scale bar represents 5 μm.

cellular concentration, Bub1 saturates the multiple phosphorylated MELT repeats of Knl1. We speculate that the increase in binding affinity promoted by the MELT1^{P}-KI1-KI2 combination increases the average occupancy over time of the MELT1 sequence but does not reflect in measurable differences in the overall kinetochore signal of Bub1, as the latter reflects binding at the many additional MELT repeats. The increase in binding affinity at MELT1, however, becomes evident under conditions of dilution and nonequilibrium associated with cell lysis and protein precipitation.

The robustness of the MELT1^{P}-KI1-KI2 constellation of motifs is also evident when testing the ability of the single MELT1 sequence to sustain the checkpoint after fusion of Knl1$^{1–250}$ to the kinetochore-targeting domain at the C terminus of Knl1. In

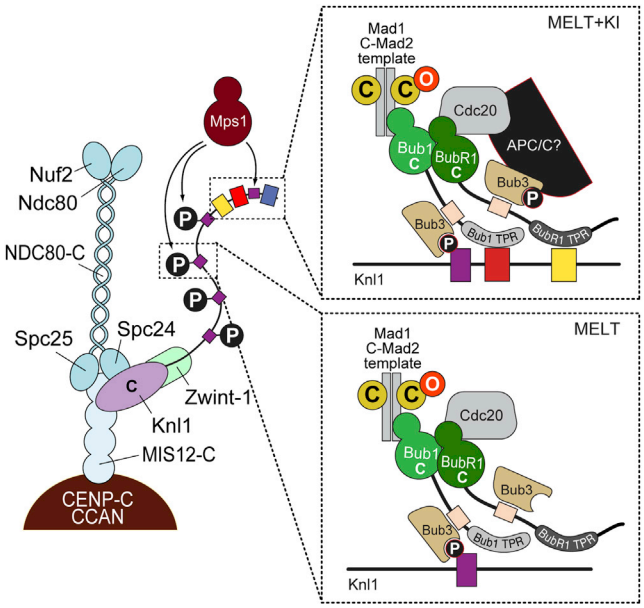

Figure 7. Model Summarizing Role of MELT, KI1, and KI2 Motifs

After phosphorylation by Mps1, MELT repeats of Knl1 become assembly stations for spindle assembly checkpoint (SAC) complexes. By binding to Bub1 and BubR1, the KI1 and KI2 motifs support the formation of a particularly robust complex of SAC proteins around MELT1^{P}. Formation of this assembly depends on Bub1 (Figure 3C). Docking of the BubR1 TPR region to the KI2 motif and an additional interaction of BubR1 with Bub1 at an unknown site stabilize the position of BubR1. Bub1 in turn recruits the Mad1/Mad2 template, which further recruits O-Mad2 to convert it into C-Mad2, which later binds Cdc20 [57]. In this model, Bub3 bound to BubR1 remains available to interact with other phosphorylated sequences. These may include other MELT repeats in Knl1 or MELT-like sequences present in other proteins, including the anaphase-promoting complex/cyclosome (APC/C). Other MELT^{P} motifs in Knl1 promote the formation of qualitatively similar complexes. Due to the lack of KI motifs near these MELT^{P}, we hypothesize that such interactions may turn over more rapidly. Recruitment of BubR1 is now largely or even exclusively mediated by the interaction of BubR1 with Bub1 at a yet-to-be-identified site.

this case, the presence of KI1 and KI2 is important for a robust checkpoint response, suggesting that the occupancy of the MELT1 site influences the strength of the checkpoint signal it contributes to produce. As enhancers of the function of the ubiquitous MELT motifs, the KI1 and KI2 motifs might serve the purpose of limiting the evolutionary expansion of MELT repeats in Knl1.

As the TPR region of Bub1 is conserved across species, in strong contrast with the KI motifs, it is unlikely that KI binding is the unique function of the TPR domain of Bub1. Rather, the Bub1 TPR might engage in other interactions with downstream partners of Bub1 [31, 50, 58]. Remarkably, we were able to precipitate Knl1$^{1–250}$ not only with Bub3, Bub1, and BubR1 but also with other checkpoint components, including Mad1, Mad2, and Cdc20. The exact order of recruitment of these components is not certain. Bub1 is required for the recruitment of BubR1 and Mad1 [37, 50, 59–67]. In turn, BubR1 is important for Cdc20 recruitment [68, 69]. Because the kinase activity of Bub1 might not be required for the checkpoint [50, 60, 65, 70], Bub1's role in the checkpoint is probably limited to protein interactions. The ability of Knl1$^{1–250}$ to seed comprehensive checkpoint complexes through direct binding of the Bub3/Bub1 complex points to Bub1 as a crucial scaffold for the assembly of the MCC, the checkpoint effector.

One of the crucial interactions mediated by Bub1 is with the Mad1/Mad2 complex [71, 72]. Previously, we have proposed that Mad1/Mad2 acts as a "template" to convert the open conformation of Mad2, O-Mad2, into the closed conformation C-Mad2 bound to Cdc20 [57]. Although a requirement for Bub1 in Mad1 and Mad2 localization had been established previously [37, 50], it had not been possible to isolate a single complex containing both Bub1 and Mad1. Here, we provide biochemical evidence of the existence of such a complex.

We have also recapitulated the requirement of Bub1 for BubR1 recruitment in a biochemical assay by showing that Bub3/BubR1 does not interact tightly with Knl1$^{1–250}$ when Bub1 has been depleted (Figure 3C). Thus, the binding affinity of Bub3/BubR1 for Knl1$^{1–250}$ is insufficient for a robust interaction in cells in the absence of Bub1. Although we were able to recapitulate this interaction in vitro (Figure 2E) at a BubR1 concentration of 400 nM, our in vitro reconstitution experiments suggested that the ability of Bub3 to bind MELT^{P} sequences is at least in part suppressed when Bub3 is bound to BubR1. At the specific concentrations of binding species used in our assay, we only observed binding of BubR1 to Knl1 when both the Bub3/MELT1^{P} and the BubR1-TPR/KI2 interactions were engaged at the same time (Figure 2E). We suspect therefore that Bub3/BubR1 is even less likely to bind to MELT repeats lacking flanking KI regions. Collectively, these observations suggest the existence of yet another interaction mode of BubR1 with kinetochores, distinct from those provided by the KI2 and MELT^{P} sequences. The molecular basis for such requirement is unknown, but our data suggest that Bub3/BubR1 is noncompetitive with Bub3/Bub1, and it may rather directly or indirectly associate with Bub3/Bub1 prebound to MELT^{P}. Our previous observation that a BubR1 mutant devoid of the TPR repeats decorates kinetochores effectively [49] strongly suggests that the TPR region of BubR1 is not required for the interaction with Bub1, and that it might be available for binding to KI2 of Knl1 when Bub1 is bound to the MELT1^{P}-KI1 combination. Indeed, we did not detect a direct interaction between two constructs, Bub3/Bub1$^{1–280}$ and Bub3/BubR1$^{1–571}$, in which both the Bub1 and the BubR1 TPR domains are represented (data not shown). Thus, other regions missing from these constructs are likely to be involved in the Bub1/BubR1 interaction. Understanding the precise mechanism of Bub3/BubR1 recruitment to the kinetochore is an important challenge for future studies on SAC signaling.

Experimental Procedures

Mammalian Plasmids

Plasmids were derived from the pCDNA5/FRT/TO-EGFP-IRES, a previously modified version [49] of the pCDNA5/FRT/TO vector (Invitrogen). To create all N-terminally tagged EGFP fusions, we amplified Knl1 fragments by PCR from a full-length human Knl1 cDNA (isoform 2), a gift from M. Yanagida (University of Kyoto), and subcloned them in-frame with the EGFP tag. To generate Plk4 fusions, we amplified the sequence encoding the centrosome localization domain of human Plk4 (Plk4 CLD, residues 475–970) by PCR from human PLK4, a gift from M. Bettencourt-Dias (Instituto Gulbenkian de Ciência), and cloned it into pCDNA5/FRT/TO-EGFP-IRES. Knl1 fragments were then added between GFP and Plk4 CLD. To generate C-terminally tagged KNL1-GFP constructs, we amplified the DNA sequence encoding residues 1834–2316 of Knl1 by PCR and inserted them before the GFP sequence using restriction-free cloning [73]. Sequences encoding N-terminal Knl1 fragments were then added to those encoding Knl1^{C} in sequential steps. Mutations and deletions within the KNL1-GFP constructs were generated by standard site-directed mutagenesis or by a mutagenesis protocol [74]. Knl1-expressing constructs were rendered siRNA resistant by changing the sequence targeted by HSS183683 to 5′-CACCCAATGTCAC ACTGCGAACATTCAG-3′, by HSS125942 to 5′-TCTATTGTGGAGGTGTTCT

AGACAA-3′, and by HSS125943 to 5′-CCCACTGGAAGAGTGGTCAAA CAAT-3′. All plasmids were verified by sequencing.

Additional detailed methodological information can be found in the Supplemental Experimental Procedures.

Supplemental Information

Supplemental Information includes five figures and Supplemental Experimental Procedures and can be found with this article online at http://dx.doi.org/10.1016/j.cub.2013.11.046.

Acknowledgments

We are grateful to Geert Kops and Jakob Nilsson for communicating results prior to publication; to Stefano Maffini, Jasmin Nelles, Slava Ziegler, Ingrid Hoffmann, and Anna De Antoni for support with experiments and technical suggestions; and to all members of the Musacchio laboratory for comments and discussions. V.K. is enrolled in the PhD program of the European School of Molecular Medicine (SEMM) and in the International Max Planck Research School in Chemical Biology and was generously supported by a predoctoral fellowship from Boehringer Ingelheim Fonds. K.O. is enrolled in the International Max Planck Research School in Chemical Biology. A.M. acknowledges funding from the European Union's Seventh Framework Programme ERC agreement KINCON and the Integrated Project MitoSys, and from the Italian Association for Cancer Research (AIRC).

Received: October 3, 2013
Revised: November 11, 2013
Accepted: November 25, 2013
Published: December 19, 2013

References

1. Foley, E.A., and Kapoor, T.M. (2013). Microtubule attachment and spindle assembly checkpoint signalling at the kinetochore. Nat. Rev. Mol. Cell Biol. *14*, 25–37.
2. Santaguida, S., and Musacchio, A. (2009). The life and miracles of kinetochores. EMBO J. *28*, 2511–2531.
3. Westermann, S., and Schleiffer, A. (2013). Family matters: structural and functional conservation of centromere-associated proteins from yeast to humans. Trends Cell Biol. *23*, 260–269.
4. Cheeseman, I.M., and Desai, A. (2008). Molecular architecture of the kinetochore-microtubule interface. Nat. Rev. Mol. Cell Biol. *9*, 33–46.
5. De Wulf, P., McAinsh, A.D., and Sorger, P.K. (2003). Hierarchical assembly of the budding yeast kinetochore from multiple subcomplexes. Genes Dev. *17*, 2902–2921.
6. Pinsky, B.A., Tatsutani, S.Y., Collins, K.A., and Biggins, S. (2003). An Mtw1 complex promotes kinetochore biorientation that is monitored by the Ipl1/Aurora protein kinase. Dev. Cell *5*, 735–745.
7. Obuse, C., Iwasaki, O., Kiyomitsu, T., Goshima, G., Toyoda, Y., and Yanagida, M. (2004). A conserved Mis12 centromere complex is linked to heterochromatic HP1 and outer kinetochore protein Zwint-1. Nat. Cell Biol. *6*, 1135–1141.
8. Nekrasov, V.S., Smith, M.A., Peak-Chew, S., and Kilmartin, J.V. (2003). Interactions between centromere complexes in Saccharomyces cerevisiae. Mol. Biol. Cell *14*, 4931–4946.
9. Westermann, S., Cheeseman, I.M., Anderson, S., Yates, J.R., 3rd, Drubin, D.G., and Barnes, G. (2003). Architecture of the budding yeast kinetochore reveals a conserved molecular core. J. Cell Biol. *163*, 215–222.
10. Cheeseman, I.M., Chappie, J.S., Wilson-Kubalek, E.M., and Desai, A. (2006). The conserved KMN network constitutes the core microtubule-binding site of the kinetochore. Cell *127*, 983–997.
11. Emanuele, M.J., McCleland, M.L., Satinover, D.L., and Stukenberg, P.T. (2005). Measuring the stoichiometry and physical interactions between components elucidates the architecture of the vertebrate kinetochore. Mol. Biol. Cell *16*, 4882–4892.
12. Desai, A., Rybina, S., Müller-Reichert, T., Shevchenko, A., Shevchenko, A., Hyman, A., and Oegema, K. (2003). KNL-1 directs assembly of the microtubule-binding interface of the kinetochore in C. elegans. Genes Dev. *17*, 2421–2435.
13. Liu, X., McLeod, I., Anderson, S., Yates, J.R., 3rd, and He, X. (2005). Molecular analysis of kinetochore architecture in fission yeast. EMBO J. *24*, 2919–2930.
14. Cheeseman, I.M., Niessen, S., Anderson, S., Hyndman, F., Yates, J.R., 3rd, Oegema, K., and Desai, A. (2004). A conserved protein network controls assembly of the outer kinetochore and its ability to sustain tension. Genes Dev. *18*, 2255–2268.
15. Kline, S.L., Cheeseman, I.M., Hori, T., Fukagawa, T., and Desai, A. (2006). The human Mis12 complex is required for kinetochore assembly and proper chromosome segregation. J. Cell Biol. *173*, 9–17.
16. Bailey, T.L., Boden, M., Buske, F.A., Frith, M., Grant, C.E., Clementi, L., Ren, J., Li, W.W., and Noble, W.S. (2009). MEME SUITE: tools for motif discovery and searching. Nucleic Acids Res. *37* (Web Server issue), W202–W208.
17. Petrovic, A., Pasqualato, S., Dube, P., Krenn, V., Santaguida, S., Cittaro, D., Monzani, S., Massimiliano, L., Keller, J., Tarricone, A., et al. (2010). The MIS12 complex is a protein interaction hub for outer kinetochore assembly. J. Cell Biol. *190*, 835–852.
18. Maskell, D.P., Hu, X.-W., and Singleton, M.R. (2010). Molecular architecture and assembly of the yeast kinetochore MIND complex. J. Cell Biol. *190*, 823–834.
19. Hornung, P., Maier, M., Alushin, G.M., Lander, G.C., Nogales, E., and Westermann, S. (2011). Molecular architecture and connectivity of the budding yeast Mtw1 kinetochore complex. J. Mol. Biol. *405*, 548–559.
20. Screpanti, E., De Antoni, A., Alushin, G.M., Petrovic, A., Melis, T., Nogales, E., and Musacchio, A. (2011). Direct binding of Cenp-C to the Mis12 complex joins the inner and outer kinetochore. Curr. Biol. *21*, 391–398.
21. Przewloka, M.R., Venkei, Z., Bolanos-Garcia, V.M., Debski, J., Dadlez, M., and Glover, D.M. (2011). CENP-C is a structural platform for kinetochore assembly. Curr. Biol. *21*, 399–405.
22. Perpelescu, M., and Fukagawa, T. (2011). The ABCs of CENPs. Chromosoma *120*, 425–446.
23. Kiyomitsu, T., Iwasaki, O., Obuse, C., and Yanagida, M. (2010). Inner centromere formation requires hMis14, a trident kinetochore protein that specifically recruits HP1 to human chromosomes. J. Cell Biol. *188*, 791–807.
24. Ciferri, C., Pasqualato, S., Screpanti, E., Varetti, G., Santaguida, S., Dos Reis, G., Maiolica, A., Polka, J., De Luca, J.G., De Wulf, P., et al. (2008). Implications for kinetochore-microtubule attachment from the structure of an engineered Ndc80 complex. Cell *133*, 427–439.
25. Wei, R.R., Sorger, P.K., and Harrison, S.C. (2005). Molecular organization of the Ndc80 complex, an essential kinetochore component. Proc. Natl. Acad. Sci. USA *102*, 5363–5367.
26. Wang, H.-W., Long, S., Ciferri, C., Westermann, S., Drubin, D., Barnes, G., and Nogales, E. (2008). Architecture and flexibility of the yeast Ndc80 kinetochore complex. J. Mol. Biol. *383*, 894–903.
27. DeLuca, J.G., Gall, W.E., Ciferri, C., Cimini, D., Musacchio, A., and Salmon, E.D. (2006). Kinetochore microtubule dynamics and attachment stability are regulated by Hec1. Cell *127*, 969–982.
28. Wei, R.R., Al-Bassam, J., and Harrison, S.C. (2007). The Ndc80/HEC1 complex is a contact point for kinetochore-microtubule attachment. Nat. Struct. Mol. Biol. *14*, 54–59.
29. Espeut, J., Cheerambathur, D.K., Krenning, L., Oegema, K., and Desai, A. (2012). Microtubule binding by KNL-1 contributes to spindle checkpoint silencing at the kinetochore. J. Cell Biol. *196*, 469–482.
30. Welburn, J.P.I., Vleugel, M., Liu, D., Yates, J.R., 3rd, Lampson, M.A., Fukagawa, T., and Cheeseman, I.M. (2010). Aurora B phosphorylates spatially distinct targets to differentially regulate the kinetochore-microtubule interface. Mol. Cell *38*, 383–392.
31. Kiyomitsu, T., Obuse, C., and Yanagida, M. (2007). Human Blinkin/AF15q14 is required for chromosome alignment and the mitotic checkpoint through direct interaction with Bub1 and BubR1. Dev. Cell *13*, 663–676.
32. Pagliuca, C., Draviam, V.M., Marco, E., Sorger, P.K., and De Wulf, P. (2009). Roles for the conserved spc105p/kre28p complex in kinetochore-microtubule binding and the spindle assembly checkpoint. PLoS ONE *4*, e7640.
33. Kiyomitsu, T., Murakami, H., and Yanagida, M. (2011). Protein interaction domain mapping of human kinetochore protein Blinkin reveals a consensus motif for binding of spindle assembly checkpoint proteins Bub1 and BubR1. Mol. Cell. Biol. *31*, 998–1011.
34. Lara-Gonzalez, P., Westhorpe, F.G., and Taylor, S.S. (2012). The spindle assembly checkpoint. Curr. Biol. *22*, R966–R980.
35. McAinsh, A.D., Meraldi, P., Draviam, V.M., Toso, A., and Sorger, P.K. (2006). The human kinetochore proteins Nnf1R and Mcm21R are

required for accurate chromosome segregation. EMBO J. *25*, 4033–4049.

36. Martin-Lluesma, S., Stucke, V.M., and Nigg, E.A. (2002). Role of Hec1 in spindle checkpoint signaling and kinetochore recruitment of Mad1/Mad2. Science *297*, 2267–2270.
37. Liu, S.-T., Rattner, J.B., Jablonski, S.A., and Yen, T.J. (2006). Mapping the assembly pathways that specify formation of the trilaminar kinetochore plates in human cells. J. Cell Biol. *175*, 41–53.
38. Miller, S.A., Johnson, M.L., and Stukenberg, P.T. (2008). Kinetochore attachments require an interaction between unstructured tails on microtubules and Ndc80(Hec1). Curr. Biol. *18*, 1785–1791.
39. Fava, L.L., Kaulich, M., Nigg, E.A., and Santamaria, A. (2011). Probing the in vivo function of Mad1:C-Mad2 in the spindle assembly checkpoint. EMBO J. *30*, 3322–3336.
40. Liu, D., Vleugel, M., Backer, C.B., Hori, T., Fukagawa, T., Cheeseman, I.M., and Lampson, M.A. (2010). Regulated targeting of protein phosphatase 1 to the outer kinetochore by KNL1 opposes Aurora B kinase. J. Cell Biol. *188*, 809–820.
41. Nijenhuis, W., von Castelmur, E., Littler, D., De Marco, V., Tromer, E., Vleugel, M., van Osch, M.H., Snel, B., Perrakis, A., and Kops, G.J. (2013). A TPR domain-containing N-terminal module of MPS1 is required for its kinetochore localization by Aurora B. J. Cell Biol. *201*, 217–231.
42. Yamagishi, Y., Yang, C.-H., Tanno, Y., and Watanabe, Y. (2012). MPS1/Mph1 phosphorylates the kinetochore protein KNL1/Spc7 to recruit SAC components. Nat. Cell Biol. *14*, 746–752.
43. Schittenhelm, R.B., Chaleckis, R., and Lehner, C.F. (2009). Intrakinetochore localization and essential functional domains of Drosophila Spc105. EMBO J. *28*, 2374–2386.
44. Shepperd, L.A.L., Meadows, J.C.J., Sochaj, A.M.A., Lancaster, T.C.T., Zou, J.J., Buttrick, G.J.G., Rappsilber, J.J., Hardwick, K.G.K., and Millar, J.B.A.J. (2012). Phosphodependent recruitment of Bub1 and Bub3 to Spc7/KNL1 by Mph1 kinase maintains the spindle checkpoint. Curr. Biol. *22*, 891–899.
45. London, N., Ceto, S., Ranish, J.A., and Biggins, S. (2012). Phosphoregulation of Spc105 by Mps1 and PP1 regulates Bub1 localization to kinetochores. Curr. Biol. *22*, 900–906.
46. Rosenberg, J.S., Cross, F.R., and Funabiki, H. (2011). KNL1/Spc105 recruits PP1 to silence the spindle assembly checkpoint. Curr. Biol. *21*, 942–947.
47. Meadows, J.C., Shepperd, L.A., Vanoosthuyse, V., Lancaster, T.C., Sochaj, A.M., Buttrick, G.J., Hardwick, K.G., and Millar, J.B.A. (2011). Spindle checkpoint silencing requires association of PP1 to both Spc7 and kinesin-8 motors. Dev. Cell *20*, 739–750.
48. Bolanos-Garcia, V.M., Lischetti, T., Matak-Vinković, D., Cota, E., Simpson, P.J., Chirgadze, D.Y., Spring, D.R., Robinson, C.V., Nilsson, J., and Blundell, T.L. (2011). Structure of a Blinkin-BUBR1 complex reveals an interaction crucial for kinetochore-mitotic checkpoint regulation via an unanticipated binding Site. Structure *19*, 1691–1700.
49. Krenn, V., Wehenkel, A., Li, X., Santaguida, S., and Musacchio, A. (2012). Structural analysis reveals features of the spindle checkpoint kinase Bub1-kinetochore subunit Knl1 interaction. J. Cell Biol. *196*, 451–467.
50. Klebig, C., Korinth, D., and Meraldi, P. (2009). Bub1 regulates chromosome segregation in a kinetochore-independent manner. J. Cell Biol. *185*, 841–858.
51. Taylor, S.S., Ha, E., and McKeon, F. (1998). The human homologue of Bub3 is required for kinetochore localization of Bub1 and a Mad3/Bub1-related protein kinase. J. Cell Biol. *142*, 1–11.
52. Primorac, I., Weir, J.R., Chiroli, E., Gross, F., Hoffmann, I., van Gerwen, S., Ciliberto, A., and Musacchio, A. (2013). Bub3 reads phosphorylated MELT repeats to promote spindle assembly checkpoint signaling. Elife *2*, e01030.
53. Tighe, A., Staples, O., and Taylor, S. (2008). Mps1 kinase activity restrains anaphase during an unperturbed mitosis and targets Mad2 to kinetochores. J. Cell Biol. *181*, 893–901.
54. Saurin, A.T., van der Waal, M.S., Medema, R.H., Lens, S.M.A., and Kops, G.J.P.L. (2011). Aurora B potentiates Mps1 activation to ensure rapid checkpoint establishment at the onset of mitosis. Nat. Commun. *2*, 316–319.
55. Santaguida, S., Vernieri, C., Villa, F., Ciliberto, A., and Musacchio, A. (2011). Evidence that Aurora B is implicated in spindle checkpoint signalling independently of error correction. EMBO J. *30*, 1508–1519.
56. Santaguida, S., Tighe, A., D'Alise, A.M., Taylor, S.S., and Musacchio, A. (2010). Dissecting the role of MPS1 in chromosome biorientation and the spindle checkpoint through the small molecule inhibitor reversine. J. Cell Biol. *190*, 73–87.
57. De Antoni, A., Pearson, C.G., Cimini, D., Canman, J.C., Sala, V., Nezi, L., Mapelli, M., Sironi, L., Faretta, M., Salmon, E.D., and Musacchio, A. (2005). The Mad1/Mad2 complex as a template for Mad2 activation in the spindle assembly checkpoint. Curr. Biol. *15*, 214–225.
58. Vanoosthuyse, V., Valsdottir, R., Javerzat, J.-P., and Hardwick, K.G. (2004). Kinetochore targeting of fission yeast Mad and Bub proteins is essential for spindle checkpoint function but not for all chromosome segregation roles of Bub1p. Mol. Cell. Biol. *24*, 9786–9801.
59. Logarinho, E., Resende, T., Torres, C., and Bousbaa, H. (2008). The human spindle assembly checkpoint protein Bub3 is required for the establishment of efficient kinetochore-microtubule attachments. Mol. Biol. Cell *19*, 1798–1813.
60. Perera, D., Tilston, V., Hopwood, J.A., Barchi, M., Boot-Handford, R.P., and Taylor, S.S. (2007). Bub1 maintains centromeric cohesion by activation of the spindle checkpoint. Dev. Cell *13*, 566–579.
61. Millband, D.N.D., and Hardwick, K.G.K. (2002). Fission yeast Mad3p is required for Mad2p to inhibit the anaphase-promoting complex and localizes to kinetochores in a Bub1p-, Bub3p-, and Mph1p-dependent manner. Mol. Cell. Biol. *22*, 2728–2742.
62. Meraldi, P., and Sorger, P.K. (2005). A dual role for Bub1 in the spindle checkpoint and chromosome congression. EMBO J. *24*, 1621–1633.
63. Essex, A., Dammermann, A., Lewellyn, L., Oegema, K., and Desai, A. (2009). Systematic analysis in Caenorhabditis elegans reveals that the spindle checkpoint is composed of two largely independent branches. Mol. Biol. Cell *20*, 1252–1267.
64. Yamamoto, T.G., Watanabe, S., Essex, A., and Kitagawa, R. (2008). SPDL-1 functions as a kinetochore receptor for MDF-1 in Caenorhabditis elegans. J. Cell Biol. *183*, 187–194.
65. Sharp-Baker, H., and Chen, R.H. (2001). Spindle checkpoint protein Bub1 is required for kinetochore localization of Mad1, Mad2, Bub3, and CENP-E, independently of its kinase activity. J. Cell Biol. *153*, 1239–1250.
66. Gillett, E.S., Espelin, C.W., and Sorger, P.K. (2004). Spindle checkpoint proteins and chromosome-microtubule attachment in budding yeast. J. Cell Biol. *164*, 535–546.
67. Vigneron, S., Prieto, S., Bernis, C., Labbé, J.-C., Castro, A., and Lorca, T. (2004). Kinetochore localization of spindle checkpoint proteins: who controls whom? Mol. Biol. Cell *15*, 4584–4596.
68. Li, D., Morley, G., Whitaker, M., and Huang, J.-Y. (2010). Recruitment of Cdc20 to the kinetochore requires BubR1 but not Mad2 in Drosophila melanogaster. Mol. Cell. Biol. *30*, 3384–3395.
69. Malureanu, L., Jeganathan, K.B., Jin, F., Baker, D.J., van Ree, J.H., Gullon, O., Chen, Z., Henley, J.R., and van Deursen, J.M. (2010). Cdc20 hypomorphic mice fail to counteract de novo synthesis of cyclin B1 in mitosis. J. Cell Biol. *191*, 313–329.
70. Fernius, J., and Hardwick, K.G. (2007). Bub1 kinase targets Sgo1 to ensure efficient chromosome biorientation in budding yeast mitosis. PLoS Genet. *3*, e213.
71. Brady, D.M., and Hardwick, K.G. (2000). Complex formation between Mad1p, Bub1p and Bub3p is crucial for spindle checkpoint function. Curr. Biol. *10*, 675–678.
72. Kim, S., Sun, H., Tomchick, D.R., Yu, H., and Luo, X. (2012). Structure of human Mad1 C-terminal domain reveals its involvement in kinetochore targeting. Proc. Natl. Acad. Sci. USA *109*, 6549–6554.
73. Bond, S.R., and Naus, C.C. (2012). RF-Cloning.org: an online tool for the design of restriction-free cloning projects. Nucleic Acids Res. *40* (Web Server issue), W209–W213.
74. Liu, H., and Naismith, J.H. (2008). An efficient one-step site-directed deletion, insertion, single and multiple-site plasmid mutagenesis protocol. BMC Biotechnol. *8*, 91.